

University of Edinburgh 96/9
University of Liverpool LTH-376
hep-lat/9607014

Soft Covariant Gauges on the Lattice

UKQCD Collaboration

D.S. Henty, O. Oliveira, C. Parrinello¹ and S. Ryan

Department of Physics and Astronomy, University of Edinburgh, Edinburgh
EH9 3JZ, Scotland

Abstract

We present an exploratory study of a one-parameter family of covariant, non-perturbative lattice gauge-fixing conditions, that can be implemented through a simple Monte Carlo algorithm. We demonstrate that at the numerical level the procedure is feasible, and as a first application we examine the gauge dependence of the gluon propagator.

¹Present address: Dept. of Mathematical Sciences, University of Liverpool, Liverpool L69 3BX, U.K.

1 Introduction

In recent years, hadron spectroscopy has become the most popular field of application of lattice QCD. Hadron masses, decay constants and matrix elements for semileptonic decays are routinely computed from Green functions of composite hadron fields and expectation values of current operators between hadron states. However, the predictive power of lattice QCD is not limited to these kinds of calculations. In particular, Green functions of individual quark and gluon fields can be computed as well as expectation values of operators between quark and gluon states. The interest of this approach is twofold. Firstly, one can non-perturbatively compute renormalisation constants for composite operators by sandwiching them between quark states [1]. These calculations form a crucial step in extracting physical information from lattice calculations. Secondly, quark and gluon Green functions are interesting objects in their own right. Being the most fundamental computable quantities in QCD, they are expected to contain direct information on the mechanism of colour confinement and chiral symmetry breaking. Also, they allow a direct determination from first principles of the running QCD coupling [2] and may be relevant for understanding the physics of pomeron exchange from the point of view of QCD [3].

Unlike hadronic operators, Green functions for quark and gluons must be defined in a fixed gauge. For most of the applications described above, it is a crucial problem to disentangle gauge dependent features from gauge independent ones. For example, if a dynamical mass were extracted from a nonperturbative study of the gluon propagator, a physical interpretation may be attached to it only if one can obtain reasonable evidence that such a mass does not depend on the gauge chosen, at least within a class of gauges. For this reason, it would be of great interest to be able to define and implement on the lattice a whole family of nonperturbative gauge conditions, by varying continuously some gauge parameter.

In this paper we describe a numerical study of one such class of gauges. In section 2 we recall the formulation of the gauge condition, in the framework of the Feynman path integral, and the corresponding Monte Carlo algorithm. In Section 3 we discuss the numerical performance of the algorithm and we present a preliminary study of the gauge dependence of the gluon propagator. Finally, In Section 4 we sketch our agenda for the future.

2 Global Gauge-Fixing

2.1 General Framework

We start from Wilson's lattice gauge model, defined by the gauge invariant partition function:

$$Z_W \equiv \int dU e^{-\beta S_W[U]}, \quad (1)$$

where $\beta = \frac{1}{g^2 N}$ for a gauge group $SU(N)$ and S_W is the standard Wilson action. The formula for the expectation value of an observable O is:

$$\langle O \rangle_W = Z_W^{-1} \int dU e^{-\beta S_W[U]} O[U]. \quad (2)$$

It is well known (Elitzur's theorem) that if $O[U]$ is a local, gauge dependent function the above expression vanishes.

In [4] a general procedure for nonperturbative lattice gauge-fixing was proposed. They defined a modified partition function by simply inserting a factor 1 in (1):

$$Z_{mod} \equiv \int dU e^{-\beta S_W[U]} I^{-1}[U] \int dg e^{-\beta M^2 F[U^g]}, \quad (3)$$

where the dg integration runs over the group of lattice gauge transformations. $F[U^g]$ is a generic function of the links such that it is not invariant under general gauge transformations and $I[U]$ is defined as

$$I[U] \equiv \int dg e^{-\beta M^2 F[U^g]}. \quad (4)$$

Clearly $I[U]$ is gauge invariant. As usual, the gauge-transformed link is defined as

$$U_\mu^g(n) \equiv g(n) U_\mu(n) g^\dagger(n + \mu). \quad (5)$$

Formula (3) corresponds to the first step of the standard Faddeev-Popov gauge-fixing procedure. However, unlike what would happen in the continuum, $Z_{mod} \equiv Z_W$ is a finite quantity because the group of gauge transformations on a finite lattice is compact. Thus Z_{mod} can provide a new definition for the expectation value of $O[U]$:

$$\langle O \rangle_{mod} \equiv Z_{mod}^{-1} \int dU e^{-\beta S_W[U]} I^{-1}[U] \int dg e^{-\beta M^2 F[U^g]} O[U^g]. \quad (6)$$

In general, if $O[U]$ is gauge dependent its expectation value in the modified scheme does not vanish. If $O[U]$ is gauge invariant then $\langle O \rangle_W = \langle O \rangle_{mod}$, so that (6) defines a consistent, nonperturbative gauge-fixing procedure.

By defining

$$\langle O[U] \rangle_G \equiv I^{-1}[U] \int dg e^{-\beta M^2 F[U^g]} O[U^g], \quad (7)$$

$\langle O \rangle_{mod}$ can be cast in the form:

$$\langle O \rangle_{mod} = \frac{\int dU e^{-\beta S_W[U]} \langle O[U] \rangle_G}{\int dU e^{-\beta S_W[U]}} = \langle \langle O[U] \rangle_G \rangle_W. \quad (8)$$

The above expression indicates that in the gauge-fixed model the expectation value of a gauge dependent quantity $O[U]$ is obtained in two steps. First one

associates with $O[U]$ the gauge invariant function $\langle O[U] \rangle_G$, which has the form of a Gibbs average of $O[U^g]$ over the group of gauge transformations, with a statistical weight factor $e^{-\beta M^2 F[U^g]}$. Then one takes the average of $\langle O[U] \rangle_G$ *a la* Wilson.

This suggests the following numerical algorithm:

1. generate a set of link configurations U_1, \dots, U_N , weighted by the Wilson action, via the usual gauge invariant Monte Carlo algorithm for some value of β ;
2. use each of the U_i as a set of quenched “bonds” in a new Monte Carlo process, where the dynamical variables are the local gauge group elements $g(n)$ located on the lattice sites. These are coupled through the links U_i , according to the effective Hamiltonian $F[U_i^g]$. In this way one can produce for every link configuration U_i an ensemble of gauge-related configurations, weighted by the Boltzmann factor $\exp(-\beta M^2 F[U_i^g])$. We call $\langle O[U_i] \rangle_G$ the average of a gauge dependent observable O with respect to such an ensemble, in the spirit of Formula (8).
3. Finally, the expectation value $\langle O \rangle_{mod}$ is simply obtained from the Wilson average of the $\langle O[U_i] \rangle_G$, i.e.:

$$\langle O \rangle_{mod} \approx \frac{1}{N} \sum_{i=1}^N \langle O[U_i] \rangle_G . \quad (9)$$

In the above scheme M^2 can be interpreted as a gauge parameter, which determines the effective temperature $1/\beta M^2$ of the Monte Carlo on the group of gauge transformations. In the following we will refer to such a Monte Carlo process as GFMC. The goal of our project is to simulate the system for many different values of M^2 , corresponding to different gauge choices. This would enable us to study the gauge dependence of relevant lattice quantities.

2.2 A Convenient Class of Gauges

For our numerical study we will use the gauge-fixing function

$$F[U^g] \equiv - \sum_{n, \mu} \text{Re Tr}(U_\mu^g(n)), \quad (10)$$

where the sum runs over all lattice links. There are many motivations for such a choice. Recalling (5), it turns out that as an effective Hamiltonian for the GFMC process the above function describes a simple nearest-neighbour interaction of the variables $g(n)$, with couplings given by the corresponding (quenched) links. The $g(n)$ can be interpreted as $SU(3)$ -valued spins, and the couplings are also

elements of $SU(3)$. In this sense (10) defines a classical, 4-dimensional $SU(3)$ spin-glass with $SU(3)$ couplings.

For small values of β and M^2 , numerical results may be compared with analytical ones, derived from a strong coupling expansion (see [4] for details). Also, a weak coupling expansion of a continuum version of this model has been performed by Fachin [5]. The latter, which is valid for any value of M^2 , may prove extremely useful when investigating the continuum limit of our lattice system.

Besides practical advantages, the choice (10) also has a theoretical interest as the continuum version of this class of gauges [6] was proposed as a possible solution to the Gribov problem in the Landau gauge [7]. Landau gauge-fixing has similar features on the lattice and in the continuum formulation of the theory. In particular, it has been shown that Gribov copies also exist on the lattice [8]. The connection of such a scheme with the Landau gauge appears when one studies the behaviour of (10) as a function of the g variables, for fixed U . Then it turns out that the stationary points of $F[U^g]$ correspond to link configurations U^g that satisfy the lattice version of the Landau gauge condition. All such configurations correspond to Gribov copies. In particular, those corresponding to local minima of $F[U^g]$ also satisfy a positivity condition for the lattice Faddeev-Popov operator [9]. As a consequence, in the limit $M^2 \rightarrow \infty$, the above gauge-fixing is equivalent to the so-called minimal Landau gauge condition, which prescribes to pick up on every gauge orbit the field configuration corresponding to the absolute minimum of $F[U^g]$ [10]. We will not discuss the Gribov problem in further detail, as it is not central to our present purpose. Here our main goal is to determine whether the above scheme for lattice gauge-fixing can be efficiently simulated numerically.

3 Numerical Results

3.1 Performance of the Algorithm and Thermodynamics

For our exploratory study we considered quenched QCD on a 8^4 lattice at $\beta = 5.7$. All the numerical work was performed on single-processor Alpha workstations, located at the University of Edinburgh. We first generated link configurations, weighted by the Wilson action, using a hybrid-overrelaxed algorithm, where both the Cabibbo-Marinari (CM) pseudo-heat-bath and overrelaxed (OR) updates were performed on three $SU(2)$ subgroups. Next, as described in the previous section, for each link configuration we produced an ensemble of gauge-related configurations, weighted by the Boltzmann factor $\exp(-\beta M^2 F[U^g])$. This was done for many different values of βM^2 and again the GFMC sweep was a combination of CM and OR updates.

Before analysing the above system we studied a simpler one, for testing purposes. This was obtained by setting all the link variables to the identity, corresponding to the limit $\beta \rightarrow \infty$, and then generating “pure gauge” configura-

tions, weighted by $\exp(-M^2 F[I^g])$. The resulting system has the form of a four-dimensional $SU(3)$ spin model with ferromagnetic couplings. We examined its thermodynamics in view of a comparison with the three-dimensional case, which has been studied in the literature [11]. We found evidence for a first order phase transition, at $M^2 = 1/T = 0.635$. This was obtained by studying the M^2 -dependence of the specific heat of the system, defined as

$$C_G = \frac{1}{M^2} \frac{dE}{d(M^2)} = \langle E^2 \rangle_G - \langle E \rangle_G^2. \quad (11)$$

where $E = F[I^g]$ and the gauge group average is defined according to (7). In the three-dimensional case a first order transition was also observed by Kogut and collaborators.

Turning to the system at $\beta = 5.7$, we analysed a range of values for M^2 up to $\beta M^2 = 2.4$. The first problem that we addressed was the study of the thermalisation of the GFMC process. In fact, by recalling the analogy of $F[U^g]$ with a spin-glass Hamiltonian, one expects metastable states to appear at low temperature (i.e. for large M^2). From the point of view of the algorithm one has to make sure that, for a chosen range of values of M^2 , the stochastic process can efficiently visit all the states and does not get trapped in a metastable one. To this end we chose one of the link configurations and performed several GFMC runs on it, using different seeds for the random number generator. For each value of M^2 at least four different seeds were used. We then analysed the evolution in GFMC time of two observables. One was the expectation value of $F[U^g]$, corresponding to the average energy of the system $\langle E[U] \rangle_G$ (cfr. Eq. (7)), the other being the zero-momentum gluon 2-point function, whose precise definition will be given in the following subsection. The important point here is that while the former quantity is a local one, the latter depends on the dynamics of long-wavelength modes of the system. For this reason we used the 2-point function to measure the autocorrelation time of our algorithm. When plotting the evolution of the observables against the number of sweeps, metastable states could be identified as the occurrence of “false” plateaux, i.e. long-lived stable values that eventually “decay” into the real vacuum. One example is shown in Fig.1, which is a plot of the zero momentum gluon 2-point function vs. the number of sweeps. At this stage, by changing the number of CM and OR updates in the GFMC sweep, we were able to optimise the performance of the algorithm at every value of M^2 , in order to get rid of metastable states. In general we found that by increasing the ratio of OR vs. CM moves the algorithm became more efficient. In the high temperature region, $\beta M^2 < 0.8$, a GFMC sweep composed of one CM sweep and two OR updates resulted in an autocorrelation time of the order of one GFMC sweep. For $\beta M^2 \geq 0.8$ we had to increase the number of OR updates, finally setting the GFMC sweep to be a combination of 1 CM and 10 OR updates. This resulted in an autocorrelation time of the order of 4 sweeps.

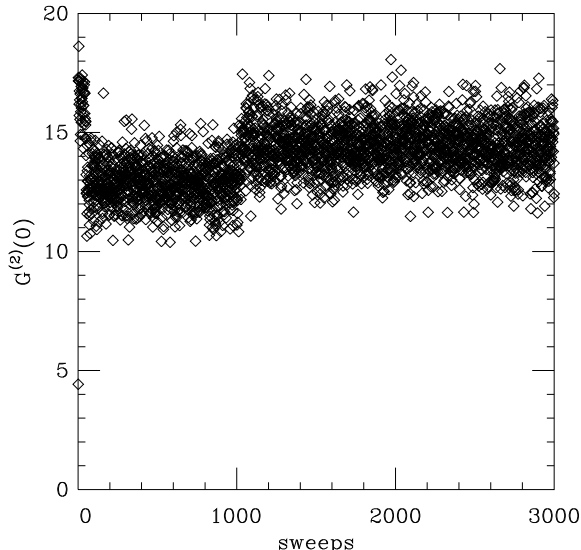


Figure 1: zero momentum gluon 2-point function vs. GFM sweeps in a typical thermalisation run.

In summary, we were able to tune the algorithm so as to obtain reasonable evidence that for $\beta M^2 \leq 2.4$ the GFM process could thermalise correctly. A similar analysis for other link configurations confirmed the pattern found with the one used for tuning. We then performed a detailed study of the thermodynamics. As expected from the behaviour of the algorithm, two separate regions in the parameter space could be identified, corresponding to a strong coupling regime for $\beta M^2 < 0.8$, and a weak coupling one, for $\beta M^2 \geq 0.8$. A phase transition seems to separate them. The nature of the transition was analysed again in terms of the specific heat, defined now as

$$C_{mod} = \frac{1}{\beta M^2} \frac{dE}{d(\beta M^2)} = \langle E^2 \rangle_{mod} - \langle E \rangle_{mod}^2, \quad (12)$$

(see Fig.2). Notice that in (12) the average is also taken with respect to link configurations (cfr. Eq. (9)). The transition still appeared to be first order, as in the ferromagnetic case, and seemed to occur for the same value of the critical temperature.

In the weak coupling region our numerical data are obtained from 21 link configurations. For each of them an ensemble of 60 gauge-related configurations was generated. In the strong coupling region the statistics is smaller. Statistical errors, obtained from a jackknife analysis, are shown in Figs.2-5. However, in most cases such error is negligible.

Fig.3 shows our numerical results for $\langle E \rangle_{mod}$ vs. βM^2 and the corresponding analytical result from a strong coupling expansion up to next to leading order [4]. The agreement is perfect up to $\beta M^2 \approx 0.7$.

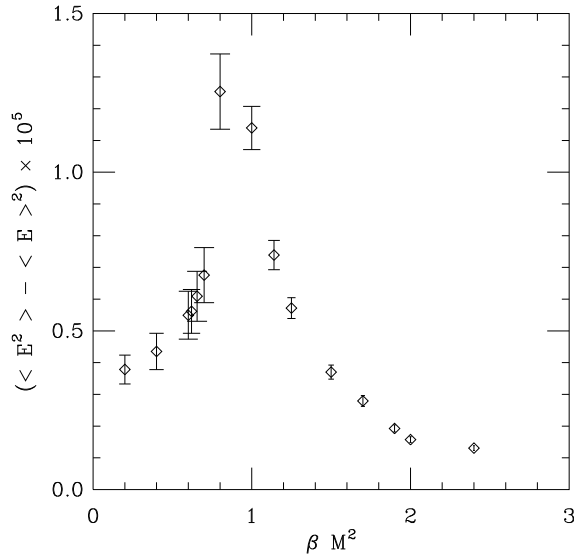


Figure 2: specific heat vs. βM^2 .

3.2 Gauge Dependence of the Gluon Propagator

Having gained confidence that we could correctly generate ensembles of gauge-related configurations for a significant range of M^2 values, we attempted a study of the gluon propagator. This quantity has been extensively studied at the non-perturbative level both in the continuum, mainly through Schwinger-Dyson equations [12], and numerically on the lattice [13].

One issue of particular relevance is the behaviour of the propagator for momenta $p \approx 0$. It has been advocated that nonperturbative effects dynamically generate a gluon mass which removes the infrared pole of the perturbative propagator. More generally, a behaviour softer than a pole has been advocated by many authors. Lattice studies seem to provide some support for the mass generation hypothesis [13], but one important point is the possible gauge dependence of such a mass. Within the limits of a preliminary investigation, we attempted to gain some insight into this issue by computing the propagator for several values of M^2 .

We recall the lattice definition of the gluon field in terms of the link variables [14],

$$A_\mu(x) = \frac{U_\mu(x) - U_\mu^\dagger(x)}{2ia g_0} - \frac{1}{3} \text{Tr} \left(\frac{U_\mu(x) - U_\mu^\dagger(x)}{2ia g_0} \right), \quad (13)$$

where a is the lattice spacing and g_0 is the bare coupling constant. By Fourier transforming the above field, one can define the bare lattice n-point gluon Green functions, in momentum space:

$$G_{\mu_1 \mu_2 \dots \mu_n}^{(n)}(p_1, p_2, \dots, p_n) = \langle A_{\mu_1}(p_1) A_{\mu_2}(p_2) \dots A_{\mu_n}(p_n) \rangle_{mod}, \quad (14)$$

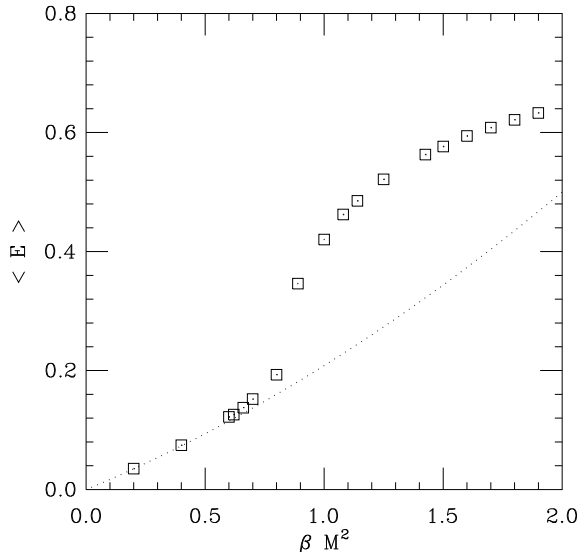


Figure 3: $\langle E \rangle_{mod}$ vs. βM^2 . The dotted line is the result from the strong coupling expansion.

where $\langle \cdot \rangle_{mod}$ obviously indicates the average according to (9) and momentum conservation implies $p_1 + p_2 + \dots + p_n = 0$.

The gluon propagator is then defined as

$$G_{\mu_1\mu_2}^{(2)}(p) = \langle A_{\mu_1}(p)A_{\mu_2}(-p) \rangle_{mod}. \quad (15)$$

In particular, we studied the following quantity:

$$G_{scalar}^{(2)}(p) = \sum_{\mu=1,4} \langle A_{\mu}(p)A_{\mu}(-p) \rangle_{mod}. \quad (16)$$

As discussed in the previous section, a comparison of our results for finite values of M^2 with those obtained in the minimal Landau gauge was of particular interest, as this gauge corresponds to the $M^2 \rightarrow \infty$ limit of our scheme. Strictly speaking, a numerical implementation of the minimal Landau gauge is not feasible on the lattice as it would require finding the absolute minimum of a spin-glass-like Hamiltonian. In practice, we assumed that the role of multiple minima could be neglected, i.e. we identified the minimal Landau gauge with the gauge obtained by imposing that $F[U^g]$ attained a local minimum. Such an approximation has been widely used in the literature [13].

In Fig.4 we plot $G_{scalar}^{(2)}(p)$ vs. p in lattice units, for a range of values of βM^2 and in the minimal Landau gauge. Our data indicate a strong dependence on the gauge parameter M^2 . In particular, for the lowest value of βM^2 , which sits on the phase transition, the propagator is essentially momentum independent, being dominated by a large effective mass generated by thermal fluctuations.

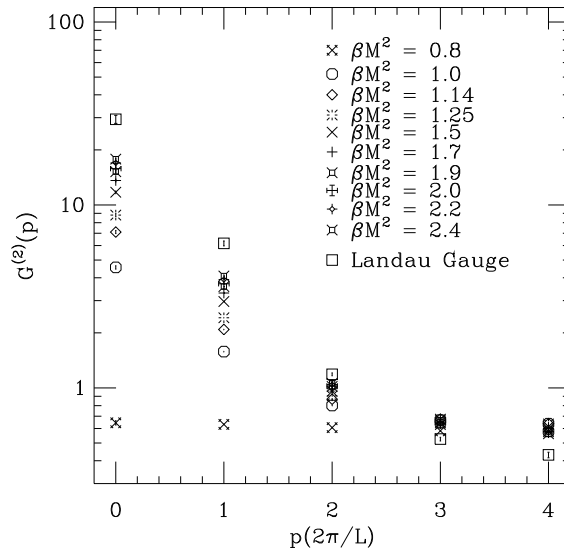


Figure 4: gluon propagator vs. momentum, for various values of βM^2 , and in the minimal Landau gauge.

Focusing on the behaviour at $p = 0$, we show in Fig.5 $G_{scalar}^{(2)}(p = 0)$ as a function of βM^2 . The dotted line indicates the Landau gauge value. Again, the M^2 -dependence appears quite substantial and strongly correlated with the phase transition, as expected. $G_{scalar}^{(2)}(p = 0)$ appears to increase monotonically with M^2 towards the minimal Landau gauge asymptotic value.

Before drawing any firm conclusion from our results we need to address the issue of the existence of the continuum limit. We plan to investigate this point in the near future by repeating our calculation for different values of β . In particular, by defining a renormalised gluon propagator as in [2], one should be able to check that such a quantity does not depend on β , for fixed M^2 .

In this connection, it should be observed that at the numerical level one does not expect our scheme to survive the continuum limit for all values of M^2 . On one hand, since in the limit $M^2 \rightarrow 0$ the gauge-fixing effect disappears, we expect the signal-to-noise ratio for a gauge dependent quantity to get worse with decreasing M^2 , with the average value eventually approaching zero. This is consistent with the data in Figs.3-5. Obviously one does not expect the scheme to have a continuum limit for values of βM^2 in the strong coupling region, where in fact the gluon propagator is suppressed by thermal fluctuations (see Figs.4-5). On the other hand, for large values of M^2 we may face increasing difficulties in the thermalisation process, so that in practice one hopes that a significant range of values of M^2 will remain accessible when increasing β .

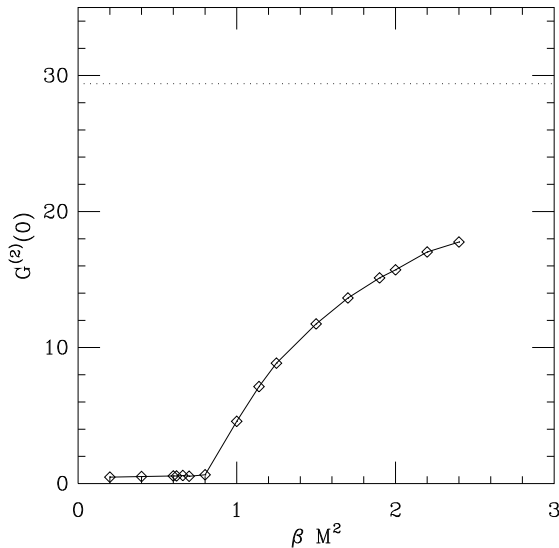


Figure 5: gluon propagator at $p = 0$ vs. βM^2 .

4 Conclusions

We have performed a preliminary numerical study of a nonperturbative lattice gauge-fixing scheme, where a whole class of gauges can be implemented by varying a gauge parameter. An efficient algorithm was devised and tested against analytical results in the strong coupling region. As a first application we studied the gauge dependence of the gluon propagator, which appears to be quite substantial, in particular at zero momentum. This preliminary result, if confirmed in a more complete analysis, would suggest that no physical meaning could be attached to a dynamically generated gluon mass. In order to establish the relevance of our results to continuum physics, we plan to increase the range of values for the gauge-fixing parameter and to repeat our calculation for higher values of β and larger lattices. Such a study will be presented in a future publication.

Acknowledgements

This work was supported by the United Kingdom Particle Physics and Astronomy Research Council (PPARC) under grant GR/J21347. OO acknowledges support from JNICT, grant BD/2714/93, CP acknowledges support from PPARC through an Advanced Fellowship held at the University of Liverpool Since September 1995 and SR acknowledges support from the FCO and the British Council. We thank A. Irving for reading the manuscript.

References

- [1] G. Martinelli, C. Pittori, C.T. Sachrajda, M. Testa, A. Vladikas, Nucl. Phys. B445 (1995) 81.
- [2] B. Alles, D. Henty, H. Panagopoulos, C. Parrinello and C. Pittori, LTH-367, hep-lat 9605033, submitted to Nucl. Phys. B.
- [3] D. Henty, C. Parrinello, D. G. Richards, Phys. Lett. B369 (1996) 130.
C. Parrinello, D. G. Richards, J. Skullerud, work in progress.
- [4] S. Fachin, C. Parrinello, Phys. Rev. D44 (1991) 2558.
- [5] S. Fachin, Phys. Rev. D47 (1993) 3487.
- [6] C. Parrinello, G. Jona-Lasinio, Phys. Lett. B251 (1990) 175.
D. Zwanziger, Nucl. Phys. B345 (1990) 461.
- [7] V. N. Gribov, Nucl. Phys. B139 (1978) 1.
- [8] E. Marinari, C. Parrinello, R. Ricci, Nucl. Phys. B362 (1991) 487.
- [9] D. Zwanziger, Phys. Lett. B257 (1991) 168.
- [10] See, for example, G. Dell'Antonio and D. Zwanziger, *All Gauge Orbits and Some Gribov Copies Encompassed by the Gribov Horizon*, in the proceedings of the workshop on *Probabilistic Methods in Quantum Field Theory and Quantum Gravity*, Cargese 1989, and references therein.
- [11] J.Kogut, M.Snow and M.Stone, Nucl. Phys. B 200 (1982) 211.
- [12] See, for example, U. Habel et al., Z. Phys. A336 (1990) 435.
- [13] See for example P. Marenzoni, G. Martinelli, N. Stella, Nucl.Phys. B455 (1995) 339.
C. Bernard, C. Parrinello, A. Soni, Phys. Rev. D49 (1994) 1585.
- [14] J. Mandula and M. Ogilvie, Phys. Lett. B185 (1987)